Comment on ‘Large-scale in situ permeability tensor of rocks from induced microseismicity’ by S. A. Shapiro, P. Audigane and J.-J. Royer

François H. Cornet

Geophys. J. Int. (2000) **140,** 465–469

Comment on 'Large-scale *in situ* permeability tensor of rocks from induced microseismicity' by S. A. Shapiro, P. Audigane and J.-J. Royer

François H. Cornet
Department de Sismologie, Institut de Physique du Globe de Paris, 4 *place Jussieu,* 75252 *Paris cedex* 05, *France. E-mail: cornet@ipgp.jussieu.fr*

Accepted 1999 September 15. Received 1999 August 19; in original form 1999 March 18

The paper 'Large-scale *in situ* permeability tensor of rocks from induced microseismicity' by Shapiro *et al.* (1999) (hereafter referred to as SAR99) is a follow-up of an article by Shapiro *et al.* (1997) (hereafter referred to as SHB97) entitled 'Estimating the crust permeability from fluid-injection-induced seismic emission at the KTB site'. In both papers, the analysis of the growth of the cloud of microseismic events induced by fluid injection in terms of large-scale permeability of the intact rock mass is proposed. It is assumed that microseismic events reflect zones where the pore pressure has been increased because of the fluid injection, so that the location of the front of the microseismic cloud provides a good description of the motion of the pressure front in the rock mass. The authors propose correlating the change in shape of the seismic cloud with the large-scale permeability of the undisturbed rock mass. The determination of the permeability proposed by SAR97 and SHB99 rests on three hypotheses:

(1) the fluid injection is assumed to be a point source;
(2) the material is assumed to be homogeneous with respect to its permeability;
(3) the hydraulic diffusivity, D, is assumed to be fluid-pressure-independent.

The fact that injection of fluid induces microseismic activity because of the related increase in pore pressure is well established. It has been observed both in the laboratory and *in situ*, and has often been discussed (Lockner & Byerlee 1977; Pearson 1981; Pine & Batchelor 1984; Talebi & Cornet 1987; Fehler 1989; Cornet 1992). Cornet & Yin (1995) have proposed a method to map the magnitude of the spatial pore pressure variation and have argued that induced seismicity may at least occasionally be a very poor indicator of the location of significant flow zones in granite rock masses. Their proposal was later supported by direct flow test observations (Cornet & Morin 1997).

The present comments are three-fold. First, I address the proposal by SHB97 to correlate the motion of the induced seismicity front with the large-scale intact rock mass permeability. Second, I show how the experiment conducted at Soultz in September 1993 is incompletely described by SAR99 and argue that it is improperly interpreted. Finally, I address the question of the relationship between the shape of the microseismic cloud and the principal stress directions at Soultz, because I strongly disagree with the SAR99 presentation of this point.

By definition, induced seismicity reflects the occurrence of unstable rupturing, that is, each event is associated with a process that locally modifies the rock mass properties. SAR99 argued that significant changes in permeability associated with the fluid injection remain localized near the borehole used for the injection because 'the front of significant changes of the medium propagates behind the faster triggering front of earlier microseismic events' (p. 208). Interestingly, Lockner & Byerlee (1977) have shown in the laboratory that the shape of the acoustic emission cloud associated with a fluid injection in a rock specimen depends on the flow rate. For the same applied compressive stress state and the same rock, they showed that for low flow rates the cloud reflects rupture in shear, whilst for fast flow rates the shape of the cloud reflects the growth of hydraulic fractures (fracture in tension). So, in this instance, had the technique proposed by SHB97 or SAR99 been applied, different characteristics for the hydraulic diffusivity of the rock specimen would have been obtained for the case of slow flow rate and the case of fast flow rate. I use this example to outline the fact that hydromechanical coupling is the significant parameter controlling the shape and the rate of growth of the seismic cloud. This is further exemplified by results concerning the location of induced seismicity observed during hydraulic fracturing (e.g. Warpinski *et al.* 1997). During hydraulic fracturing, the microseismic signals are associated with the percolation of fluid through the walls of the fracture. The fracture propagates continuously during the test and the shape of the microseismic cloud depends essentially on the shape of the fracture and on its growth rate, but very little on the permeability of the material. This is why the method is used for mapping the geometry of hydraulic fractures and *not* the intact rock permeability.

Accordingly, I conclude that the shape of the microseismic cloud does depend on the conditions of hydromechanical coupling. This coupling must be ignored for SHB97's proposition to be valid. When hydromechanical coupling occurs, both the point-source hypothesis and the constant homogeneous hydraulic diffusivity hypothesis are no longer valid. It may be argued that at the very onset of induced seismicity, when large-scale failure is not yet significant, the front of induced seismicity is a good marker of the pressure front. However, when coupling induces a large-scale fracturing process, as in the case of Lockner and Byerlee's experiments at slow and fast flow rates, the shape of the seismic cloud and its growth are associated with the development of the fracturing process and not with the hydraulic diffusivity of the intact rock mass.

Let us turn now to the Soultz September 1993 experiment discussed in SAR99. I know this experiment very well, for it was my proposal that lead to its being run (Cornet & Fara 1991; Cornet & Jones 1994, hereafter referred to as CJ94; Cornet *et al.* 1997, hereafter referred to as CHPE97). The injection was conducted in the open-hole section of well GPK1 between 2850 and 3400 m, that is, within a 550-m-long open-hole section (the 3400–3590 m depth interval had been sanded out in order to isolate a fault zone at around 3490 m). The injection started at a flow rate of 0.25 l s^{-1} and was progressively increased to 6 l s^{-1} within 60 hr. From then on, the flow rate was kept constant for periods of 48 hr followed by increments every other day of 6 l s^{-1}, until the injection flow rate reached 36 l s^{-1}. At this final flow rate, injection lasted 3 days (Fig. 1). In response, the wellhead pressure initially increased regularly but then progressively stabilized and was nearly constant once the flow rate reached 24 l s^{-1}. The monitoring of microseismic events showed that during the first 8 days, events were located around the borehole open-hole section with mostly radial growth of the seismic cloud and some downward growth. Upward growth started to appear once the flow rate reached 18 l s^{-1}. This has been described in detail by Jones *et al.* (1995) and is also shown by SAR99 (Fig. 3) and in Fig. 1 of this Comment. During injection, the flow distribution in the well changed drastically (CJ94; Evans *et al.* 1996) and this has not been reported properly in SAR99. While initially the flow loss in the upper 200 m of the open-hole section decreased regularly with each pressure increment and was equal to 35 per cent of the total injected flow at the end of the 18 l s^{-1} step, it reached more than 60 per cent when the flow rate was equal to 36 l s^{-1} (Fig. 2). Hence, for all periods during which the flow rate was smaller than 24 l s^{-1}, that is, for the first 200 hr, a very significant part of the flow occurred along the lower half of the well. During that time, the seismic cloud extended vertically between 2600 and 3500 m, that is, over a depth range of 900 m (compare this with the 550 m open-hole length). Correspondingly, during this early phase, it is incorrect to approximate the open-hole section of the well as a point source and to compute the distance between the injection point and

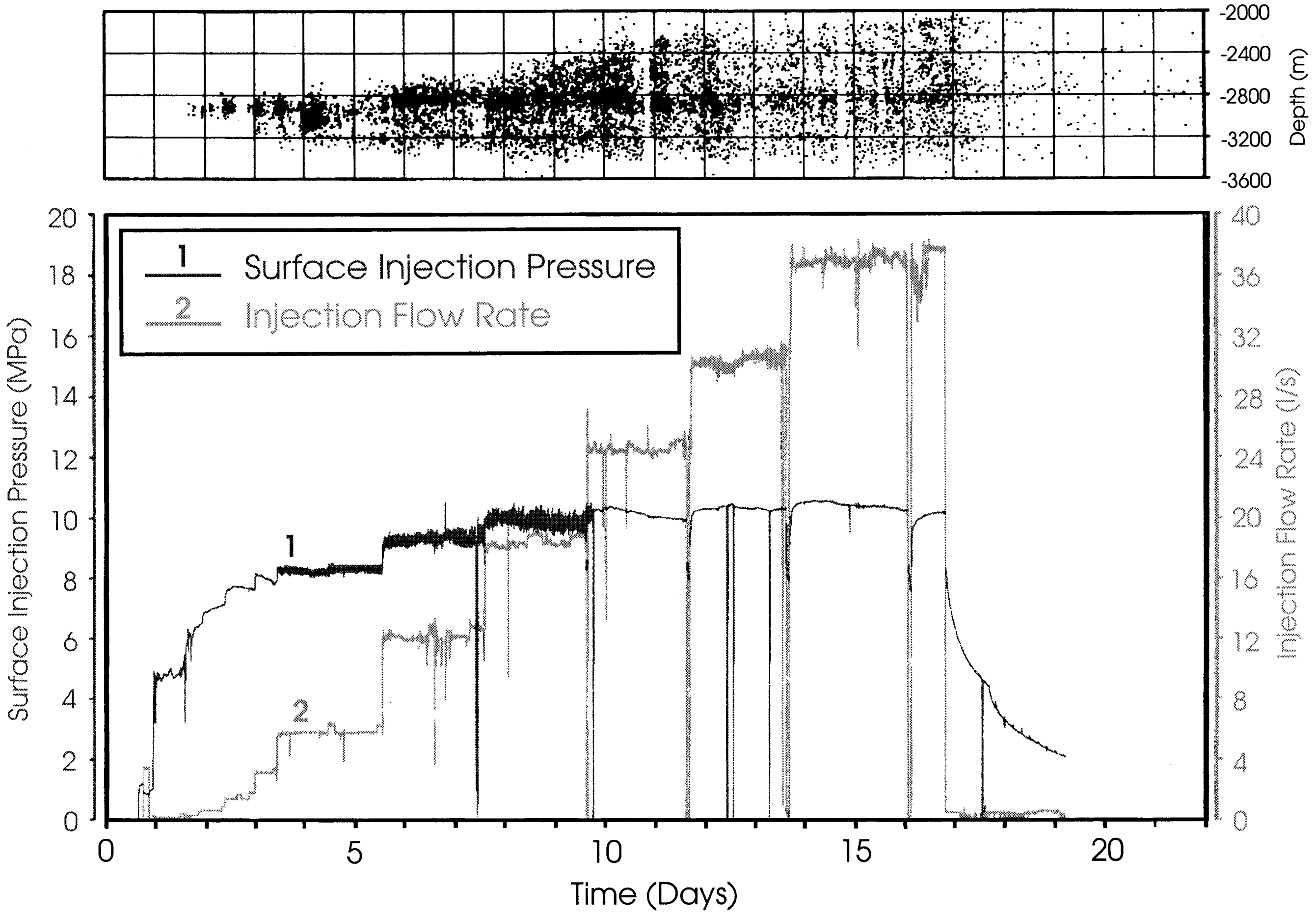

Figure 1. Injection test in GPK1: wellhead pressure and injection flow rate history. The upper part of the figure shows the depth distribution of microseismic events for the corresponding pressure and flow rate. A clear upward migration appears at the onset of the 18 l s^{-1} (1.0 MPa) step. Injection occurred through an open-hole section ranging in depth from 2850 to 3400 m, a length that is not compatible with a point-source hypothesis for the first 200 hr.

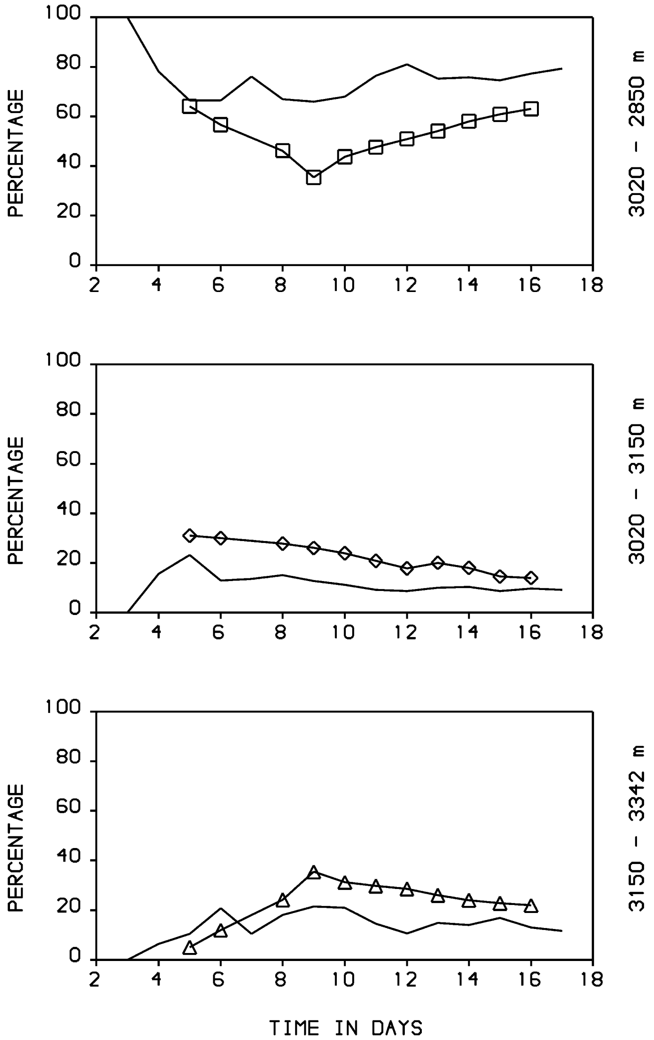

Figure 2. Relative variation of flow losses in the open-hole section compared to the depth distribution of microseismic events. The curves with squares, diamonds or triangles refer to flow losses expressed as a percentage of total injected flow as measured with a spinner tool. The continuous curves represent the percentage of microseismic events located in the corresponding depth interval. For the upper interval, the percentage concerns all events located above 3020 m depth. For the lower interval, the percentage concerns all events located below 3150 m depth. The casing shoe was at 2850 m. For the first five days flow could not be measured by the spinner tool below 3020 m but was detected by thermal logs, yet no seismicity was observed.

the observed events as the distance between the event location and the well at 2920 m depth. In reality, a line source should have been considered, so the distances between the lower seismic events and the location in the well where water percolated into the rock mass would be much smaller than that computed by SAR99. Hence, for the first 200 hr, that is, half the duration of the experiment, their Fig. 1 does not capture properly the statistics of the distances between seismic events and injection source. During the second half, when flow localized more and more in the upper part of the well, an upward growth of the seismic front was observed. However, the number of events observed between 2900 and 3500 m remained quite significant, so that, for this part of the test also, SAR99's point-source hypothesis yielded a very strong bias in their Fig. 1. Had the injection test been conducted for only 200 hr, the vertical extension of the seismic cloud would have been drastically different from that actually observed at the end of the test, so that the correlative estimate of the rock diffusivity anisotropy would have been significantly different.

I hence conclude that the vertical anisotropy described by SAR99 is very strongly biased by their point-source hypothesis and does not reflect reality. Furthermore, a significant change in hydraulic diffusivity occurred in the rock mass during the injection process, so that hypothesis 3 concerning the independence of hydraulic diffusivity with respect to pore pressure is not satisfied. Once the pore pressure becomes large enough, fracture opening occurs and flow no longer obeys a Darcy-type law. Rather, fluid motion may be approximated by flow through parallel plates, with a pressure drop within the opened fracture that is nearly insignificant compared to the values predicted by Darcy-type flow. The difficulty is in evaluating the length of the hydraulically opened fractures. As quoted by SAR99, CHPE97 has evaluated lengths of the order of 300 m (150 m radius) for opened fractures, which exhibit evidence of shear displacement at the borehole wall. However, many flowing fractures did not exhibit any permanent shear displacement so that the estimation of the length of their opened portion is left to the reader's guess.

The third point of this Comment concerns the cloud shape and its relation to the stress field. First, contrary to what is written in SAR99, the seismic cloud was oriented north–south within the volume where most of the water was lost (between 2850 and 2950 m). It was oriented more NNW–SSE in its lower portion, i.e. below 3000 m (see Fig. 6 of CHPE97, Fig. 8 of CJ94 or Fig. 6 of Jones *et al.* 1995, which is reproduced here in Fig. 3). SAR99's description is exactly opposite to these results (p. 210) and should be corrected. Also, the reference to the paper by Klee & Rummel (1993) quoted in SAR99 to specify the principal stress direction is not appropriate. Indeed, Klee & Rummel (1993) reported on results from hydraulic fracturing but stated explicitly that no data on fracture orientation were retrieved from their tests (p. 976). They only concluded that since their pressure records were similar to those reported by Rummel & Baumgärtner (1991), the principal stress directions for their stress determination were the same as those of Rummel & Baumgärtner (1991). However, interestingly, Rummel & Baumgärtner (1991), who also conducted hydraulic tests for stress determination, reported many difficulties in their testing and acknowledged that their determination of stress orientation was questionable. (The stress field was described by five parameters that were constrained by only five data points. In addition, from my point of view, the experimental procedure was also questionable because of the correlation made between depths measured with logging cable for fracture orientation determinations and depths measured with the drill string assembly for hydraulic tests.) Rummel & Baumgärtner (1991) pointed out that although they found a N130°E orientation for the maximum horizontal principal stress, a north–south direction also gave a good fit to their data. Given the observation on thermal crack orientations reported by CJ94, together with that of hydraulic fractures reported in CHPE97, the north–south orientation (actually N170°E) for the maximum horizontal principal stress seems fairly convincing. It also fits the seismic cloud orientation where flow was maximum once the pressure had stabilized (that is, the orientation of the zone in which fracture opening was expected). It has been

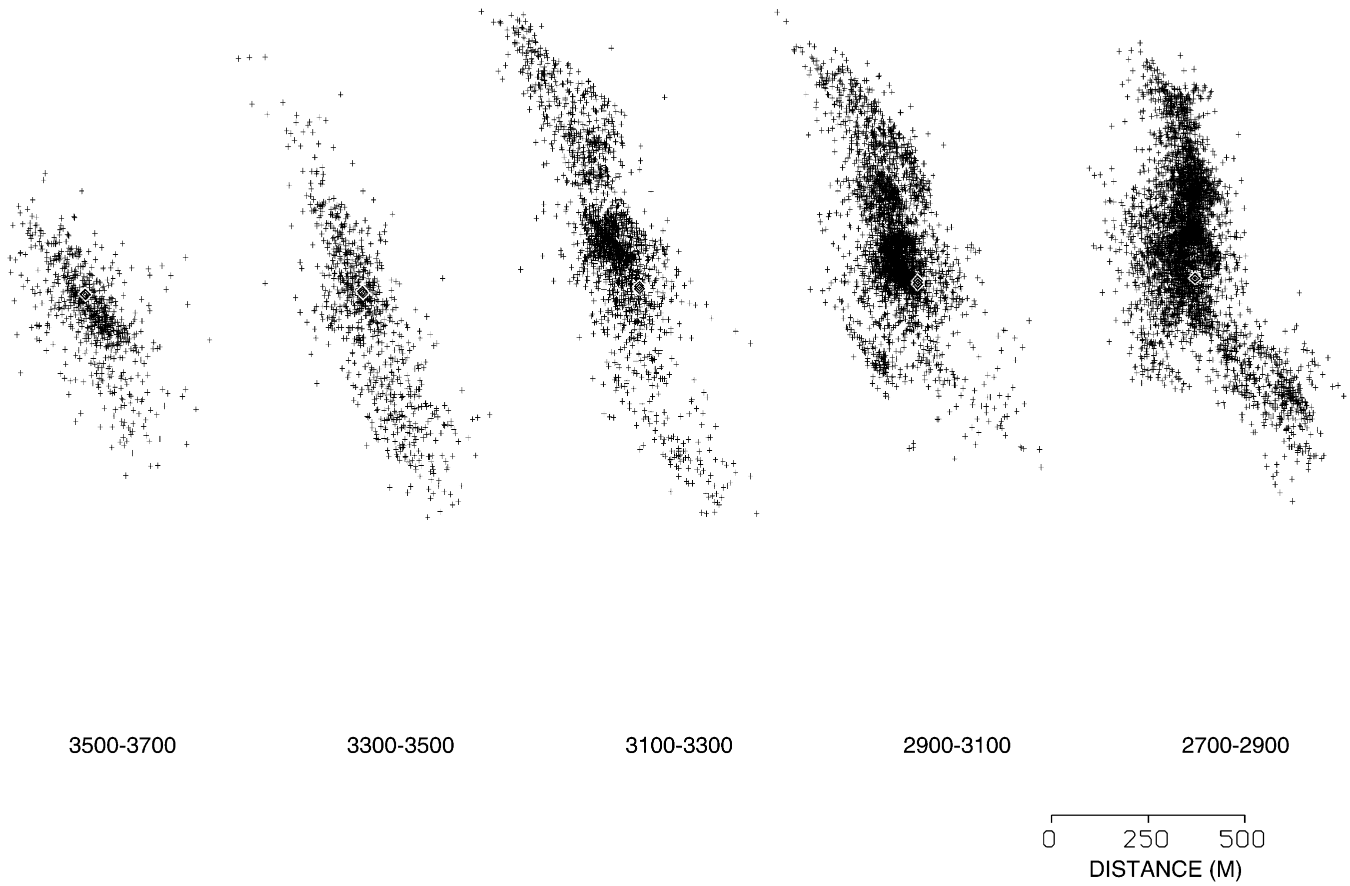

Figure 3. Projection in the horizontal plane of the location of microseismic events that occurred within the specified depth intervals. The north direction is perpendicular to the length scale indicated in the bottom right corner of the figure. The 2700–2900 m depth interval is that for which drastic changes in flow losses occurred once the well-head pressure reached 10 MPa. The small white diamonds indicate the location of the well.

argued by CHPE97 that the NNW–SSE orientation observed for the seismic cloud in its lower portion, where the flow losses were much smaller, reflects a failure of the rock mass in shear mode, so that, at a scale of about 600 m × 600 m × 600 m, the results observed at Soultz are quite similar to those obtained by Lockner & Byerlee (1977) in the laboratory.

Hence, I conclude that the shape of the seismic cloud and its growth are controlled by the fracturing process induced by the hydromechanical coupling rather than by the intact rock mass permeability.

I would like to thank S. A. Shapiro, P. Audigane and J.-J. Royer for giving me the opportunity to quote again our previously published results. CJ94 was prepared in a hurry for a panel discussion at a US Rock Mechanics symposium. A very unfortunate error was made in the caption of Fig. 5 of that paper. Indeed, the purpose of the figure was to show that the density of microseismic events per unit depth range varied with time, with a downward growth of the cloud during the initial 200 hr and an upward growth in the final stage of the test, as also reported by Jones *et al.* (1995). Thus, I take this opportunity to mention that the top diagram in Fig. 5 of CJ94 refers to the upper section of the well, whilst the lower diagram refers to the depth range below 3150 m (the opposite is stated erroneously in the figure caption). The same figure was presented by Jones *et al.* (1995). There the figure caption is correct and corresponds to Fig. 2 of the present Comment.

ACKNOWLEDGMENTS

I would like to express my sincere thanks to R. Jones and A. Mossop for their help with the figures and the review of these comments. Figs 2 and 3 are reprinted from *Rock Mechanics: Models and Measurements, Challenges from Industry—Proc. 1st North American Rock Mechanics Symposium, Austin, TX, 1–3 June 1994,* eds Nelson, P.P. & Laubach, S.E., A.A. Balkema, Rotterdam, the Netherlands.

REFERENCES

Cornet, F.H., 1992. Fracture processes induced by forced fluid percolation, in *Volcanic Seismology: IAVCEI Proc. Volcanology,* Vol. 3, pp. 407–431, eds Gasparini, P., Scarpa, R., & Aki, K., Springer-Verlag, Berlin.

Cornet, F.H. & Fara, V., 1991. Large scale pumping test in GPK1 and correlative seismic investigation, *Proposal submitted to European Community DG-XII (European Hot Dry Rock Association project)* and to *French national research program on Geothermal Energy in Deep Rocks (Geoproge).*

Cornet, F.H. & Jones, R., 1994. Field evidence on the orientation of forced water flow with respect to the regional principal stress directions; panel discussion, in *Rock Mechanics–Models and Measurements,* pp. 61–71, eds Nelson, P.P. & Laubach, S.E., Balkema, Rotterdam.

Cornet, F.H. & Morin, R., 1997. Evaluation of hydromechanical coupling in a granite rock mass from a high volume, high pressure injection experiment: Le Mayet de Montagne, France, *Int. J. Rock Mech. Min. Sci.,* **34,** No. 207.

Cornet, F.H. & Yin, J., 1995. Analysis of induced seismicity for stress field determination and pore pressure mapping, *Pageoph,* **145,** 677–700.

Cornet, F.H., Helm, J., Poitrenaud, H. & Etchecopar, A., 1997. Seismic and aseismic slips induced by large scale fluid injections, *Pageoph,* **150,** 563–583.

Evans, K.F., Kohl, T., Hopkirk, R.J. & Rybach, L., 1996. studies of the nature of non-linear impedance to flow within the fractured granitic reservoir at the European Hot Dry Rock project site at Soultz-sous-Forêts, France, *ETH–Institute of Geophysik Final Rept to Bundesamt für Bildung und Wissenschaft Projekt 93.0010,* ETH Hönggerberg, Zürich.

Fehler, M.C., 1989. Stress control of seismicity patterns observed during hydraulic fracturing experiments at the Fenton Hill hot dry rock geothermal energy site, New Mexico, *Int. J. Rock Mech. Min. Sci.,* **26,** 211–221.

Jones, R.H., Beauce, A., Jupe, A., Fabriol, H. & Dyer, B.C., 1995. Imaging induced microseismicity during the 1993 injection tests at Soultz sous Forets, France, *Proc. World Geothermal Congress, Florence, Italy,* Vol. 4, pp. 2665–2669, International Geothermal Association, San Diego.

Klee, G. & Rummel, F., 1993. Hydrofrac stress data for the European HDR research project test site Soultz-sous-Forêts, *Int. J. Rock Mech. Min. Sci,* **30,** 973–976.

Lockner, D. & Byerlee, J.D., 1977. Hydrofracture in Weber sandstone at high confining pressure and differential stress, *J. geophys. Res.,* **82,** 2018–2026.

Pearson, C., 1981. The relationship between microseismicity and high pore pressure during hydraulic stimulation experiments in low permeability granitic rocks, *J. geophys. Res.,* **86,** 7855–7864.

Pine, R.J. & Batchelor, A.S., 1984. Downward migration of shearing in jointed rock during hydraulic injections, *Int. J. Rock Mech. Min. Sci.,* **21,** 149–263.

Rummel, F. & Baumgärtner, J., 1991. Hydraulic fracturing stress measurements in the GPK-1 borehole, Soultz-sous-Forêts, *Geotherm. Sci. Tech.,* **3,** 119–148.

Shapiro, S.A., Huenges, E. & Borm, G., 1997. Estimating the crust permeability from fluid-injection-induced seismic emission at the KTB site, *Geophys. J. Int.,* **131,** F15–F18.

Shapiro, S.A., Audigane, P. & Royer, J.J., 1999. Large-scale *in situ* permeability tensor of rocks from induced microseismicity, *Geophys. J. Int.,* **137,** 207–213.

Talebi, S. & Cornet, F.H., 1987. Analysis of the microseismicity induced by a fluid injection in a granite rock mass, *Geophys. Res. Lett.,* **14,** 227–230.

Warpinski, N.R., Branagan, P.T., Engler, B.P., Wilmer, R. & Wolhart, S.L., 1997. Evaluation of a downhole tiltmeter array for monitoring hydraulic fractures, *Int. J. Rock Mech. Min. Sci.,* **34,** No. 329.